

UNSTEADY MHD OSCILLATORY FLOW OF JEFFREY FLUID, HEAT AND MASS TRANSFER BETWEEN PARALLEL PLATES WITH CHEMICAL REACTION AND HEAT SOURCE

P.R. Sharma¹ and Tripti Mehta²

^{1,2}Department of Mathematics, University of Rajasthan,
Jaipur-302004 (Raj.), India.

ABSTRACT

Aim of the paper is to investigate the effect of heat and mass transfer on unsteady MHD oscillatory flow of Jeffrey fluid between parallel plates with chemical reaction and heat source. One plate is moving and temperature prescribed at both plates is uniform and asymmetric. The effect of heat transfer on unsteady MHD oscillatory flow of fluid in vertical media are encountered in a wide range of engineering and industrial applications such as molten iron flow, recovery extraction of crude oil, geothermal systems. Numerical results for the velocity, temperature and concentration profiles for various physical parameters as well as the local skin friction coefficient, local Nusselt number and Sherwood number are discussed and presented graphically.

Keywords:

Jeffrey fluid, MHD, oscillatory flow, heat and mass transfer, chemical reaction, heat source.

1. Introduction

Oscillatory flow has known to result in higher rates of heat and mass transfer. Many studies have been done to understand its characteristics in different systems such as reciprocating engines, pulse combustors and chemical reactors. The chemical reaction effects are considered in many applications of heat and mass transfer especially those encountered in chemical reactors of porous structure, geothermal reservoirs, enhanced oil recovery etc. Researchers have considerable interest in the study of flow between two parallel plates. Because of its occurrence in rheometric experiments to determine the constitutive properties of the fluid, in lubrication engineering and in transportation and processing encountered in chemical engineering.

Bejan and Khair (1985) obtained heat and mass transfer by natural convection in a porous medium. Deka, Das and Soundalgekar (1994) studied the effect of mass transfer on flow past an impulsively started infinite vertical plate with constant heat flux and chemical reaction. Sharma and Sharma (1997) discussed unsteady flow and heat transfer between two parallel plates. Sharma and Kumar (1998) analyzed unsteady flow and heat transfer between two horizontal plates in the presence of transverse magnetic field. Acharya, Dash and Singh (2000) discussed magnetic field effects on the free convection and mass transfer flow through porous medium with constant suction and constant heat flux. Kim (2000) explained unsteady MHD convective heat transfer past a semi infinite vertical porous moving plate with variable suction. Chamkha (2003) presented MHD flow of a numerical of uniformly stretched vertical permeable surface in the presence of heat generation/absorption and chemical reaction. Sharma and Chaturvedi (2003) described unsteady flow and heat transfer of an electrically conducting viscous incompressible fluid between two non-conducting parallel porous plates under uniform transverse magnetic field.

Sharma, Chawla and Singh (2005) discussed unsteady plane Poiseuille flow and heat transfer in the presence of oscillatory temperature of the lower plate. Makinde and Mhone (2005) presented heat transfer to MHD oscillatory flow in a channel filled with porous medium. Sharma and Singh (2008) derived effects of variable thermal conductivity and heat source/sink on MHD flow near a stagnation point on a linearly stretching sheet. Pal and Talukdar (2010) obtained unsteady magnetohydrodynamic convective heat and mass transfer in a boundary layer slip flow past a vertical permeable plate with thermal radiation and chemical reaction. Israel-Cooke and Nwaigwe (2010) studied unsteady MHD flow of a radiating fluid over a moving heated porous plate with time-dependent suction. Bakr (2011) described effects of chemical reaction on MHD free convection and mass transfer flow of a micropolar fluid with oscillatory plate velocity and constant heat source in a rotating frame of reference. Shateyi and Motsa (2011) considered unsteady magnetohydrodynamic convective heat and mass transfer past an infinite vertical plate in a porous medium with thermal radiation heat generation/absorption and chemical reaction.

Kavita, Prasad and Kumari (2012) discussed slip effects on MHD oscillatory flow of Jeffrey fluid in a channel with heat transfer. Kumar, Jain and Gupta (2012) presented unsteady MHD free convection flow through porous medium sandwiched between viscous fluids. Kavita, Prasad and Kumari (2012) investigated influence of heat transfer on MHD

oscillatory flow of Jeffrey fluid in a channel. Sreenadh, Devaki and Diwakar (2012) studied unsteady flow of Jeffrey fluid in an elastic tube with stenosis. Vineet, Gupta and Varshney (2012) considered MHD effects on free convection fluid flow past a vertical surface with porous medium and radiation. Asadullah, Umar, Nareed, Raheela and Mohyuddin (2013) discussed MHD flow of a Jeffrey fluid in converging and diverging channels. Devika, Satya Narayana and Venkataramana (2013) presented MHD oscillatory flow of a visco elastic fluid in a porous channel with chemical reaction.

Aim of the paper is to investigate effects of heat and mass transfer on unsteady MHD oscillatory flow of Jeffrey fluid between parallel plates with chemical reaction and heat source. Equations of momentum, energy and diffusion, which govern the fluid flow, heat and mass transfer are solved by using perturbation method. The effects of various physical parameters on fluid velocity, temperature, concentration, skin friction coefficient, Nusselt number and Sherwood number at the plates are derived, discussed numerically and shown through graphs.

2. Mathematical analysis:

Consider an oscillatory flow of Jeffrey fluid and heat transfer through a vertical infinite channel with chemical reaction and heat source with one moving plate in the presence of transverse magnetic field. The channel width is d . Following Kavita et al., that the constitutive equation of S for Jeffrey fluid is given by

$$S = \frac{\mu}{1 + \lambda_1} \left(\frac{d\eta}{dt^*} + \lambda_2 \frac{d^2\eta}{dt^{*2}} \right),$$

...(1)

where μ the dynamic viscosity, λ_1 the ratio of relaxation to retardation times, λ_2 the retardation time, $\frac{d\eta}{dt^*}$ the shear rate and t^* the time.

The radiative heat term in horizontal direction is considered negligible in comparison with vertical direction. At time $t^* > 0$, the plate is given an impulsive motion in a horizontal direction with uniform mean velocity U . Moreover at this stage an unsteady component $\varepsilon T^* e^{i\omega t^*}$, where $\varepsilon \ll 1$ is the amplitude of oscillation, is assumed to be superimposed on the

temperatures of the plates. The x^* -axis is taken along the plate (when $y = 0$) and a straight line perpendicular to that as the y^* -axis. A magnetic field of uniform strength B_0 is applied normal to the plate along x^* -direction and the induced magnetic field is assumed negligible. It is also assumed that the fluid has small electrical conductivity and the electromagnetic force produced is very small. The pressure gradient is also assumed negligible. Since the plate is considered infinite in x^* -direction, all the physical variables will be independent of x^* and are functions of y^* and t^* . Under the usual Boussinesq's approximation, the governing equations of motion, energy and mass conservation are given by

$$\frac{\partial u^*}{\partial t^*} = -\frac{\partial P^*}{\partial x^*} + \frac{\mu}{\rho(1+\lambda_1)} \frac{\partial^2 u^*}{\partial y^{*2}} - \frac{\sigma_e B_0^2 u^*}{\rho} + g\beta_T(T^* - T_w) + g\beta_C(C^* - C_w),$$

...(2)

$$\rho C_p \frac{\partial T^*}{\partial t^*} = \kappa \frac{\partial^2 T^*}{\partial y^{*2}} - \frac{\partial q}{\partial y^*} + Q(T^* - T_w),$$

...(3)

$$\frac{\partial C^*}{\partial t^*} = D \frac{\partial^2 C^*}{\partial y^{*2}} - K_C(C^* - C_w),$$

...(4)

where u^* denotes fluid velocity along x^* -axis, t^* the time, P^* fluid pressure, T^* fluid temperature, C^* concentration of fluid, μ the dynamic viscosity, ρ fluid density, λ_1 the ratio of relaxation to retardation times, λ_2 the retardation time, σ_e electric conductivity, g acceleration due to gravity, β_T coefficient of the thermal expansion, β_C coefficient of mass expansion, κ thermal conductivity, C_p specific heat at constant pressure, q radiative heat flux in the y^* -direction, Q heat generation/ absorption constant, D the mass diffusion coefficient and K_C the chemical reaction coefficient.

The boundary conditions are given by

$$y^* = 0 : u^*(y^*, t^*) = 0, T^*(y^*, t^*) = T_w, C^*(y^*, t^*) = C_w;$$

$$y^* = d : u^*(y^*, t^*) = U_\infty(1 + \epsilon e^{i\omega t}), T^*(y^*, t^*) = T_w + (T_\infty - T_w)(1 + \epsilon e^{i\omega t}),$$

$$C^*(y^*, t^*) = C_w + (C_\infty - C_w)(1 + \epsilon e^{i\omega t}).$$

...(5)

Following Cogley et al. (1968), that the fluid is optically thin with a relative low density and radiative heat flux is given by

$$\frac{\partial q}{\partial y^*} = 4\alpha^2(T_w - T^*).$$

...(6)

Introducing the following dimensionless quantities

$$x = \frac{x^*}{d}, y = \frac{y^*}{d}, u = \frac{u^*}{U_\infty}, \theta = \frac{T^* - T_w}{T_\infty - T_w}, C = \frac{C^* - C_w}{C_\infty - C_w}, t = \frac{t^* U_\infty}{d}, \text{Re} = \frac{\rho U_\infty d}{\mu},$$

$$Ha^2 = \frac{\sigma_e B_0^2 d^2}{\mu}, Pe = \frac{\rho d U_\infty C_p}{\kappa}, N^2 = \frac{4\alpha^2 d^2}{\kappa}, J = \frac{K_c d}{U_\infty}, Sc = \frac{d U_\infty}{D}, S = \frac{Q d^2}{\kappa},$$

$$Gr = \frac{\rho d^2 g \beta_T (T_\infty - T_w)}{\mu U_\infty}, Gc = \frac{\rho d^2 g \beta_C (C_\infty - C_w)}{\mu U_\infty};$$

...(7)

into the equations (2), (3), (4), we get

$$\text{Re} \frac{\partial u}{\partial t} = \frac{1}{(1 + \lambda_1)} \frac{\partial^2 u}{\partial y^2} - Ha^2 u + Gr\theta + GcC,$$

...(8)

$$Pe \frac{\partial \theta}{\partial t} = \frac{\partial^2 \theta}{\partial y^2} + N^2 \theta + S\theta,$$

...(9)

$$\frac{\partial C}{\partial t} = \frac{1}{Sc} \frac{\partial^2 C}{\partial y^2} - JC,$$

...(10)

where u is dimensionless velocity, t the dimensionless time, y dimensionless coordinate axis normal to the plates, θ dimensionless temperature, C dimensionless concentration, Re the Reynolds number, Ha Hartmann number, Gr Grashof number, Gc modified Grashof

number, Pe Peclet number, N Radiation parameter, S heat source parameter, Sc Schmidt number and J chemical reaction parameter.

The dimensionless boundary conditions are given by

$$y = 0 : u(y,t) = 0, \theta(y,t) = 0, C(y,t) = 0;$$

$$y = 1 : u(y,t) = 1 + \varepsilon e^{i\alpha t}, \theta(y,t) = 1 + \varepsilon e^{i\alpha t}, C(y,t) = 1 + \varepsilon e^{i\alpha t}.$$

...(11)

3. Method of Solution

In order to solve equations (8), (9) and (10) under the boundary conditions (11) assuming

$$u(y,t) = u_0(y) + \varepsilon u_1(y)e^{i\alpha t} + O(\varepsilon^2),$$

$$\theta(y,t) = \theta_0(y) + \varepsilon \theta_1(y)e^{i\alpha t} + O(\varepsilon^2),$$

$$C(y,t) = C_0(y) + \varepsilon C_1(y)e^{i\alpha t} + O(\varepsilon^2),$$

...(12)

using (12) into the equations (8), (9) and (10), equating the coefficients of the harmonic and non-harmonic terms and neglecting the coefficients of ε^2 , we obtain

$$a_1^2 u_0''(y) - Ha^2 u_0(y) = -Gr\theta_0(y) - GcC_0(y),$$

...(13)

$$a_1^2 u_1''(y) - b_1^2 u_1(y) = -Gr\theta_1(y) - GcC_1(y),$$

...(14)

$$\theta_0''(y) + a_2^2 \theta_0(y) = 0,$$

...(15)

$$\theta_1''(y) + b_2^2 \theta_1(y) = 0,$$

...(16)

$$C_0''(y) - a_3^2 C_0(y) = 0,$$

...(17)

$$C_1''(y) - b_3^2 C_1(y) = 0.$$

...(18)

where $a_1^2 = \frac{1}{1 + \lambda_1}$, $b_1^2 = Ha^2 + i\omega Re$, $a_2^2 = N^2 + S$, $b_2^2 = N^2 + S - i\omega Pe$,
 $a_3^2 = K Sc$ and $b_3^2 = K Sc + i\omega Sc$.

Now, the corresponding boundary conditions are reduced to

$$y = 0: u_0(y) = 0, \theta_0(y) = 0, C_0(y) = 0; u_1(y) = 0, \theta_1(y) = 0, C_1(y) = 0;$$

$$y = 1: u_0(y) = 1, \theta_0(y) = 1, C_0(y) = 1; u_1(y) = 1, \theta_1(y) = 1, C_1(y) = 1.$$

...(19)

Equations (13) to (18) are ordinary second order differential equations and solved under the boundary conditions (19). Through straight forward calculations $u_0(y)$, $u_1(y)$, $\theta_0(y)$, $\theta_1(y)$, $C_0(y)$ and $C_1(y)$ are known. Finally, the expressions of $u(y,t)$, $\theta(y,t)$ and $C(y,t)$ are known as given below

$$u(y,t) = \left[\left(1 - \frac{Gr}{(a_1^2 a_2^2 + Ha^2)} + \frac{Gc}{(a_1^2 a_3^2 - Ha^2)} \right) \frac{\sinh p_1 y}{\sinh p_1} + \frac{Gr}{(a_1^2 a_2^2 + Ha^2)} \frac{\sin a_2 y}{\sin a_2} - \frac{Gc}{(a_1^2 a_3^2 - Ha^2)} \frac{\sinh a_3 y}{\sinh a_3} \right] + \varepsilon \left[\left(1 - \frac{Gr}{(a_1^2 b_2^2 + b_1^2)} + \frac{Gc}{(a_1^2 b_3^2 - b_1^2)} \right) \frac{\sinh q_1 y}{\sinh q_1} + \frac{Gr}{(a_1^2 b_2^2 + b_1^2)} \frac{\sin b_2 y}{\sin b_2} - \frac{Gc}{(a_1^2 b_3^2 - b_1^2)} \frac{\sinh b_3 y}{\sinh b_3} \right] e^{i\omega t},$$

...(20)

$$\theta(y,t) = \frac{\sin a_2 y}{\sin a_2} + \varepsilon \frac{\sin b_2 y}{\sin b_2} e^{i\omega t},$$

...(21)

$$C(y,t) = \frac{\sinh a_3 y}{\sinh a_3} + \varepsilon \frac{\sinh b_3 y}{\sinh b_3} e^{i\omega t},$$

...(22)

The dimensionless stress tensor in terms of skin-friction coefficient at both the plates are given by

$$C_f = \frac{du}{dy} = \frac{du_0}{dy} + \varepsilon e^{i\omega t} \frac{du_1}{dy} \text{ at } y=0 \text{ and } y=1, \dots(23)$$

Hence, skin-friction coefficient at the plate (when $y = 0$) is given by

$$\begin{aligned} (C_f)_0 = & \left[\left(1 - \frac{Gr}{(a_1^2 a_2^2 + Ha^2)} + \frac{Gc}{(a_1^2 a_3^2 - Ha^2)} \right) \frac{p_1}{\sinh p_1} + \frac{Gr}{(a_1^2 a_2^2 + Ha^2)} \frac{a_2}{\sin a_2} \right. \\ & \left. - \frac{Gc}{(a_1^2 a_3^2 - Ha^2)} \frac{a_3}{\sinh a_3} \right] + \varepsilon \left[\left(1 - \frac{Gr}{(a_1^2 b_2^2 + b_1^2)} + \frac{Gc}{(a_1^2 b_3^2 - b_1^2)} \right) \frac{q_1}{\sinh q_1} \right. \\ & \left. + \frac{Gr}{(a_1^2 b_2^2 + b_1^2)} \frac{b_2}{\sin b_2} - \frac{Gc}{(a_1^2 b_3^2 - b_1^2)} \frac{b_3}{\sinh b_3} \right] e^{i\omega t}, \dots(24) \end{aligned}$$

The skin-friction coefficient at the plate (when $y = 1$) is given by

$$\begin{aligned} (C_f)_1 = & \left[\left(1 - \frac{Gr}{(a_1^2 a_2^2 + Ha^2)} + \frac{Gc}{(a_1^2 a_3^2 - Ha^2)} \right) \frac{p_1 \cosh p_1}{\sinh p_1} + \frac{Gr}{(a_1^2 a_2^2 + Ha^2)} \frac{a_2 \cos a_2}{\sin a_2} \right. \\ & \left. - \frac{Gc}{(a_1^2 a_3^2 - Ha^2)} \frac{a_3 \cosh a_3}{\sinh a_3} \right] + \varepsilon \left[\left(1 - \frac{Gr}{(a_1^2 b_2^2 + b_1^2)} + \frac{Gc}{(a_1^2 b_3^2 - b_1^2)} \right) \frac{q_1 \cosh q_1}{\sinh q_1} \right. \\ & \left. + \frac{Gr}{(a_1^2 b_2^2 + b_1^2)} \frac{b_2 \cos b_2}{\sin b_2} - \frac{Gc}{(a_1^2 b_3^2 - b_1^2)} \frac{b_3 \cosh b_3}{\sinh b_3} \right] e^{i\omega t}. \dots(25) \end{aligned}$$

The dimensionless rate of heat transfer in terms of the Nusselt number at both the plates is given by

$$Nu = -\left(\frac{\partial \theta}{\partial y} \right) = -\left(\frac{d\theta_0}{dy} + \varepsilon e^{i\omega t} \frac{d\theta_1}{dy} \right) \text{ at } y=0 \text{ and } y=1, \dots(26)$$

Hence, the Nusselt number at the plate (when $y = 0$) is given by

$$(Nu)_0 = -\frac{a_2}{\sin a_2} - \varepsilon \frac{b_2}{\sin b_2} e^{i\omega t},$$

...(27)

The Nusselt number at the plate (when $y = 1$) is given by

$$(Nu)_1 = -\frac{a_2 \cos a_2}{\sin a_2} - \varepsilon \frac{b_2 \cos b_2}{\sin b_2} e^{i\omega t}.$$

...(28)

The dimensionless rate of mass transfer in terms of the Sherwood number at both the plates is given by

$$Sh = -\left(\frac{\partial C}{\partial y}\right) \text{ at } y = 0 \text{ and } y = 1,$$

...(29)

Hence, the Sherwood number at the plate (when $y = 0$) is given by

$$(Sh)_0 = -\frac{a_3}{\sinh a_3} - \varepsilon \frac{b_3}{\sinh b_3} e^{i\omega t},$$

...(30)

The Sherwood number at the plate (when $y = 1$) is given by

$$(Sh)_1 = -\frac{a_3 \cosh a_3}{\sinh a_3} - \varepsilon \frac{b_3 \cosh b_3}{\sinh b_3} e^{i\omega t}.$$

...(31)

4. Results and Discussions

It is observed from figure 1 that as Grashof number increases, the velocity increases. Therefore, for higher values of Grashof number the flow at the boundary is turbulent while for lower values the flow at the boundary is laminar.

Figure 2 shows that with the increase in modified Grashof number contributes to the rise in velocity of the fluid. Figure 3 illustrates that the velocity of the fluid decreases as the values of Hartmann number increases. Figure 4 reveals that velocity increases as heat source parameter. Figure 5 shows that the velocity increases as the radiation parameter. Figure 6 depicts that velocity decreases with increase in Schmidt number. Figure 7 represents that an

increase in chemical reaction parameter results in decreasing the fluid velocity. Figure 8 demonstrates that the velocity increases with increase in material parameter. The ratio of relaxation to retardation times enhances the increase flow of velocity when it becomes large.

Figure 9 shows that the increase in the heat source parameter significantly increase the thermal buoyancy effects which rise fluid temperature. Figure 10 illustrates that increase in the radiation parameter increases the fluid temperature because of large values of radiation parameter oppose the conduction over radiation, thereby which increases the buoyancy force and increases the thickness of the thermal boundary layer.

Figure 11 represents that an increase in Schmidt number results in decreasing the fluid concentration. Figure 12 shows concentration decreases for increasing the chemical reaction parameter which indicates that the diffusion rates can be tremendously changed by the chemical reaction.

It is seen from Table 1 and Table 2 that the velocity decreases with the increase in Reynolds number and Peclet number. Table 3 shows that the velocity of the fluid is inversely proportional to the frequency of the oscillation, thus increasing of frequency reduces the velocity of the fluid. It is observed from Table 4 and Table 5 that the fluid temperature decreases with increase in Peclet number and frequency of oscillation. It is noted from Table 6 that the concentration of the fluid decreases with an increase in frequency of the oscillation.

It is observed from Table 7 that the skin friction coefficient at the plate (when $y = 0$) increases due to increase in Grashof number, modified Grashof number, heat source parameter, radiation parameter or material parameter, while it decreases due to increase in Reynolds number, Hartmann number, Peclet number, Schmidt number, chemical reaction parameter or frequency of the oscillation. The skin-friction coefficient at the plate (when $y = 1$) increases due to increase of Reynolds number, Hartmann number, Peclet number, Schmidt number, chemical reaction parameter or frequency of the oscillation, while it decreases due to increase of Grashof number, modified Grashof number, heat source parameter, radiation parameter or material parameter.

It is noted from Table 8 that the Nusselt number at the plate (when $y = 0$) increases due to increase in Peclet number or frequency of the oscillation, while it decreases due to increase in heat source parameter or radiation parameter, but opposite behaviour is seen at the plate (when $y = 1$).

It is seen from Table 9 that the Sherwood number at the plate (when $y = 0$) increases due to increase in Schmidt number, chemical reaction parameter or frequency of the oscillation. The Sherwood number at the plate (when $y = 1$) increases due to increase in frequency of the oscillation, while it decreases due to increase of Schmidt number or chemical reaction parameter.

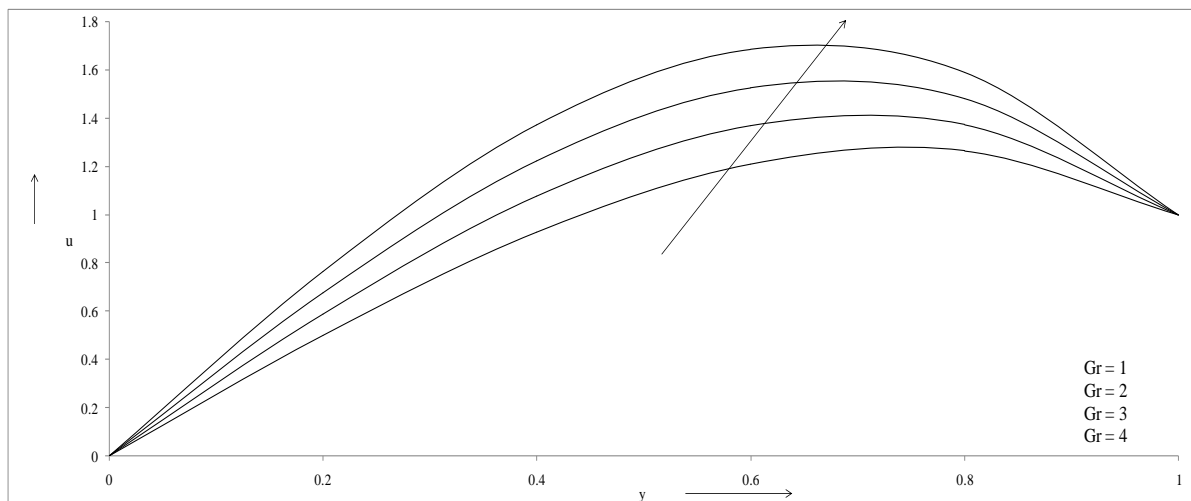


Figure 1. Velocity profiles versus y for different values of Gr when $Gc=10$, $Re=2$, $Ha=1.0$, $Pe=0.71$, $S=5.0$, $N=1.0$, $Sc=0.60$, $J=0.5$, $\omega=0.1$, $\varepsilon=0.001$, $t=0.5$, $\lambda_1=0.1$.

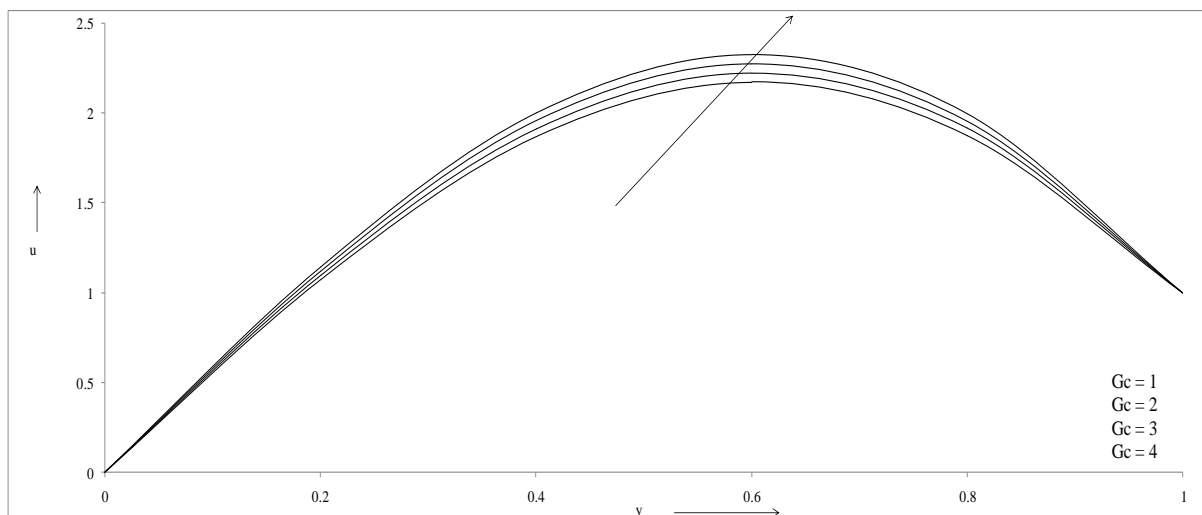


Figure 2. Velocity profiles versus y for different values of Gc when $Gr=10$, $Re=2$, $Ha=1.0$, $Pe=0.71$, $S=5.0$, $N=1.0$, $Sc=0.60$, $J=0.5$, $\omega=0.1$, $\varepsilon=0.001$, $t=0.5$, $\lambda_1=0.1$.

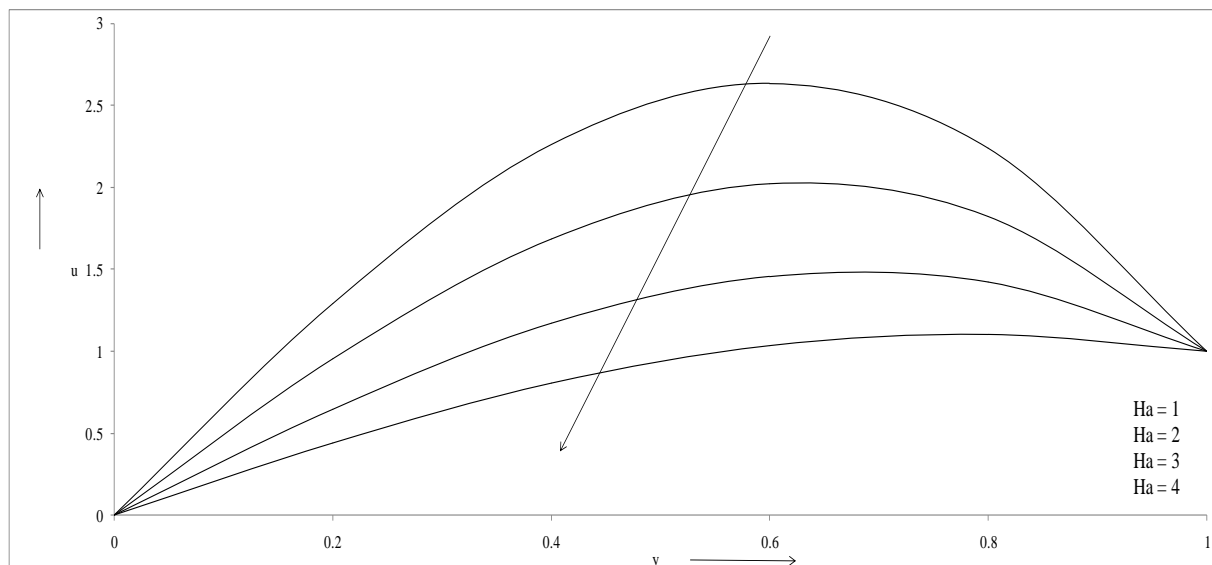


Figure 3. Velocity profiles versus y for different values of Ha when $Gr=10$, $Gc=10$, $Re=2$, $Pe=0.71$, $S=5.0$, $N=1.0$, $Sc=0.60$, $J=0.5$, $\omega=0.1$, $\varepsilon=0.001$, $t=0.5$, $\lambda_1=0.1$.

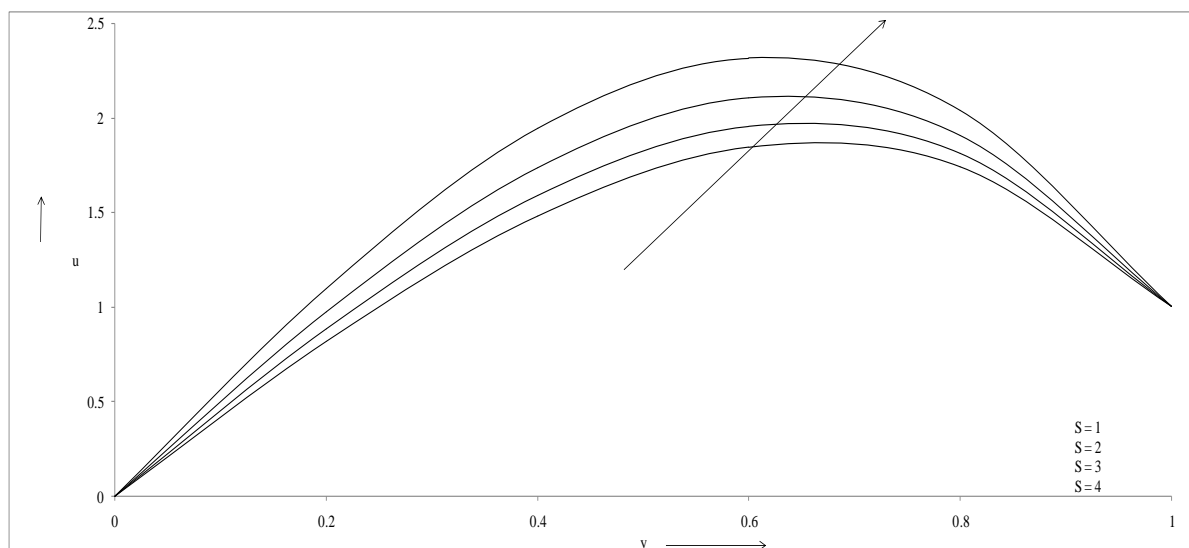


Figure 4. Velocity profiles versus y for different values of S when $Gr=10$, $Gc=10$, $Re=2$, $Ha=1.0$, $Pe=0.71$, $N=1.0$, $Sc=0.60$, $J=0.5$, $\omega=0.1$, $\varepsilon=0.001$, $t=0.5$, $\lambda_1=0.1$.

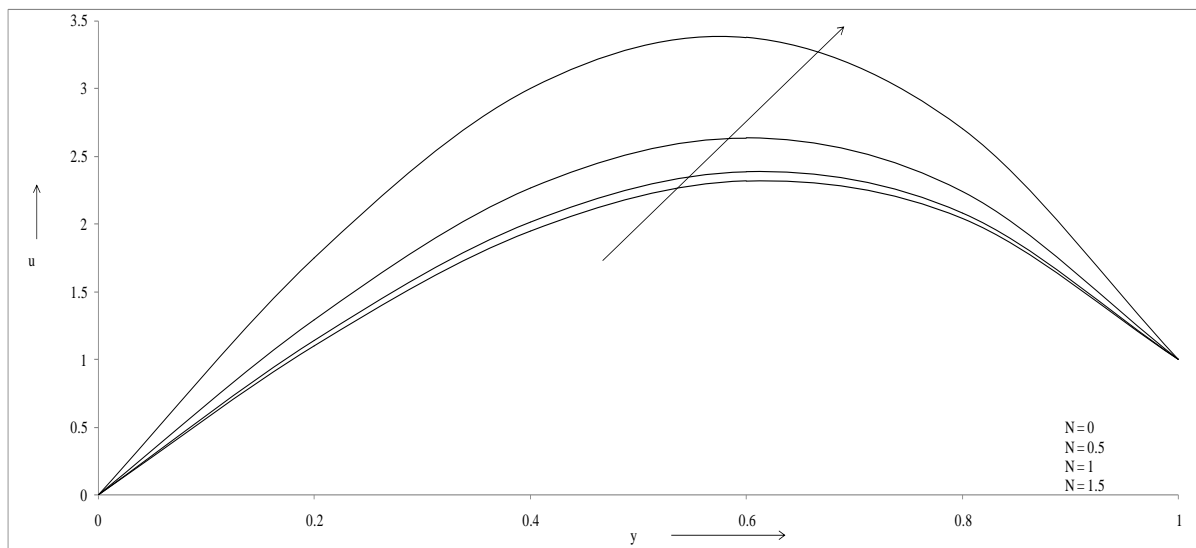


Figure 5. Velocity profiles versus y for different values of N when $Gr=10$, $Gc=10$, $Re=2$, $Ha=1.0$, $Pe=0.71$, $S=5.0$, $Sc=0.60$, $J=0.5$, $\omega=0.1$, $\varepsilon=0.001$, $t=0.5$, $\lambda_1=0.1$.

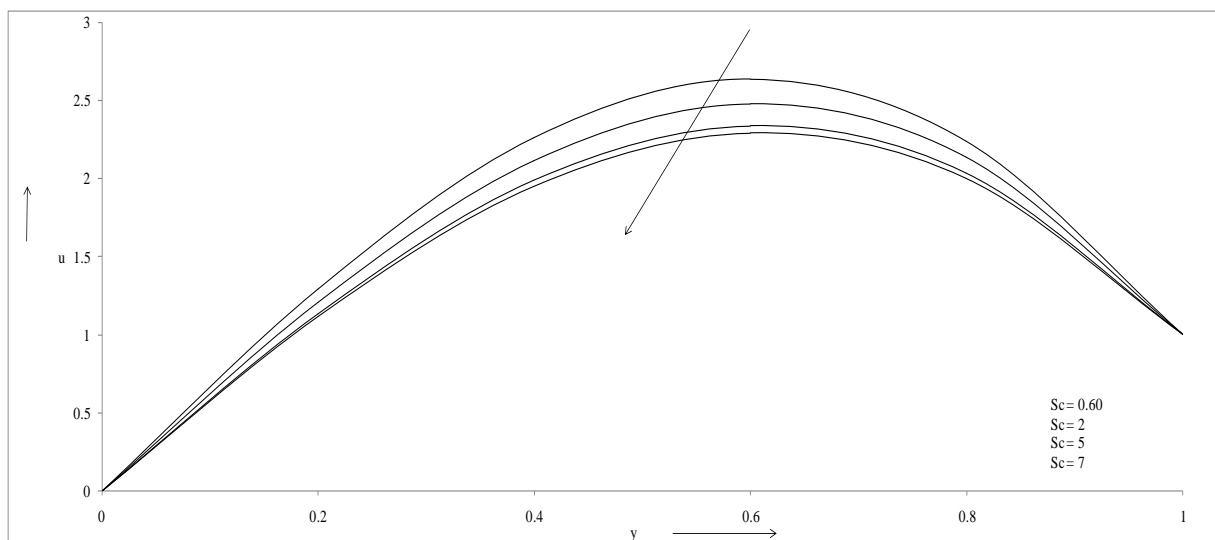


Figure 6. Velocity profiles versus y for different values of Sc when $Gr=10$, $Gc=10$, $Re=2$, $Ha=1.0$, $Pe=0.71$, $S=5.0$, $N=1.0$, $Sc=0.60$, $J=0.5$, $\omega=0.1$, $\varepsilon=0.001$, $t=0.5$, $\lambda_1=0.1$.

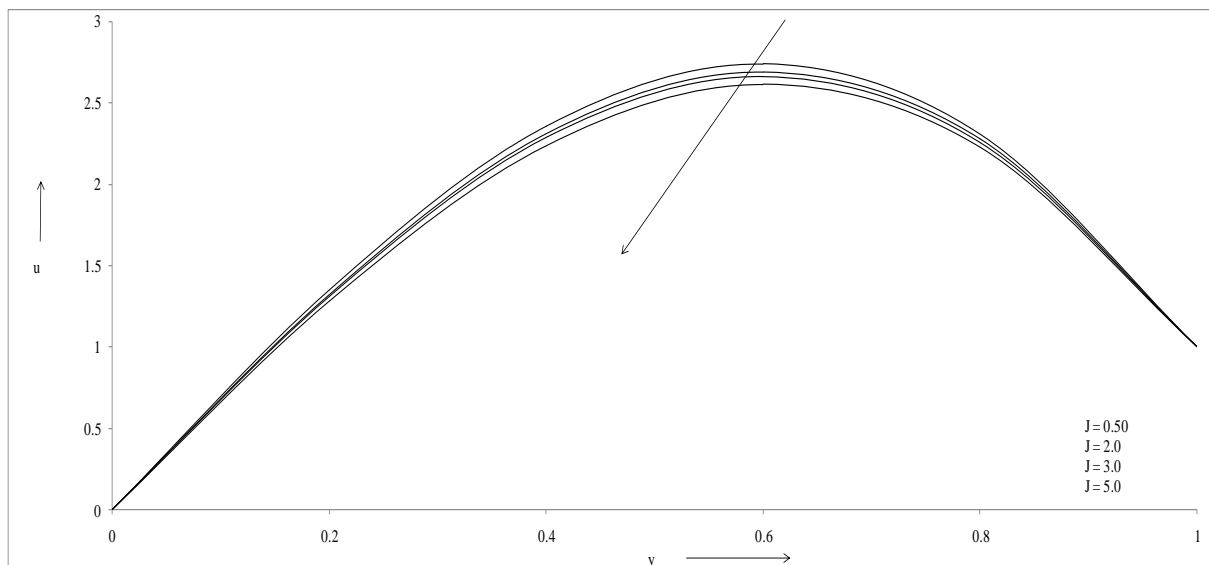


Figure 7. Velocity profiles versus y for different values of J when $Gr=10$, $Gc=10$, $Re=2$, $Ha=1.0$, $Pe=0.71$, $S=5.0$, $N=1.0$, $Sc=0.60$, $\omega=0.1$, $\varepsilon=0.001$, $t=0.5$, $\lambda_1=0.1$.

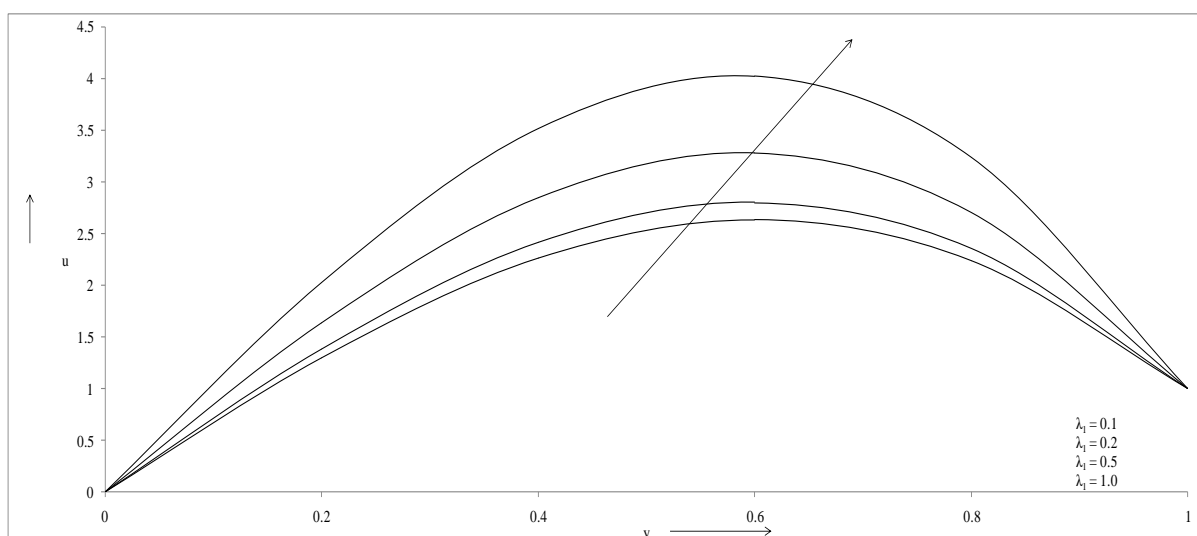


Figure 8. Velocity profiles versus y for different values of λ_1 when $Gr=10$, $Gc=10$, $Re=2$, $Ha=1.0$, $Pe=0.71$, $S=5.0$, $N=1.0$, $Sc=0.60$, $J=0.5$, $\omega=0.1$, $\varepsilon=0.001$, $t=0.5$.

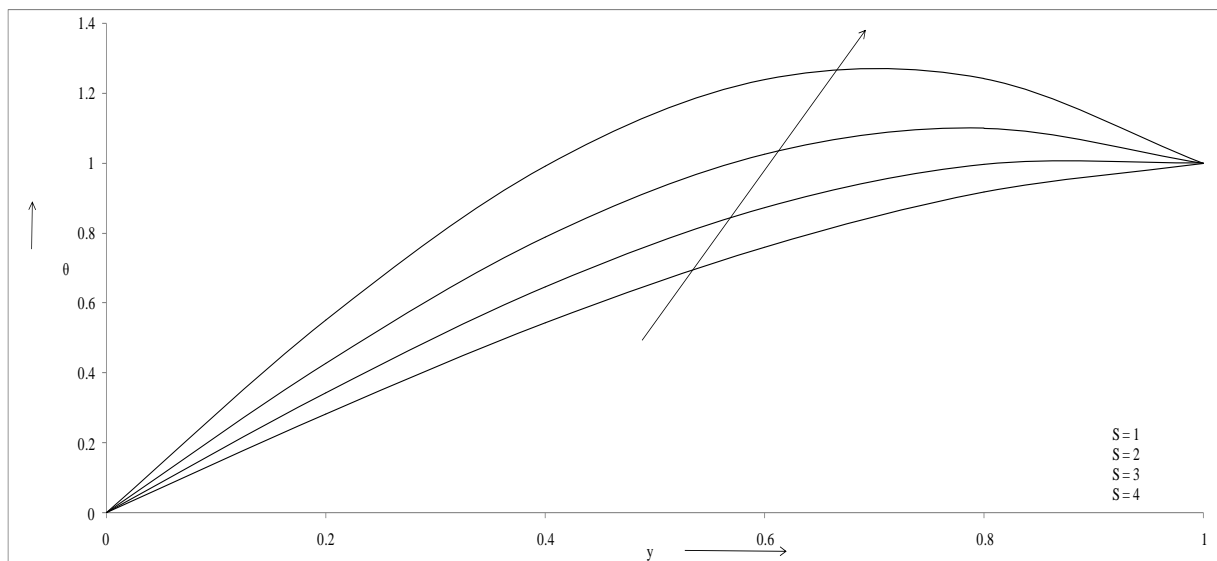


Figure 9. Temperature profiles versus y for different values of S when $Gr=10$, $Gc=10$, $Re=2$, $Ha=1.0$, $Pe=0.71$, $N=1.0$, $Sc=0.60$, $J=0.5$, $\omega=0.1$, $\epsilon=0.001$, $t=0.5$, $\lambda_1=0.1$.

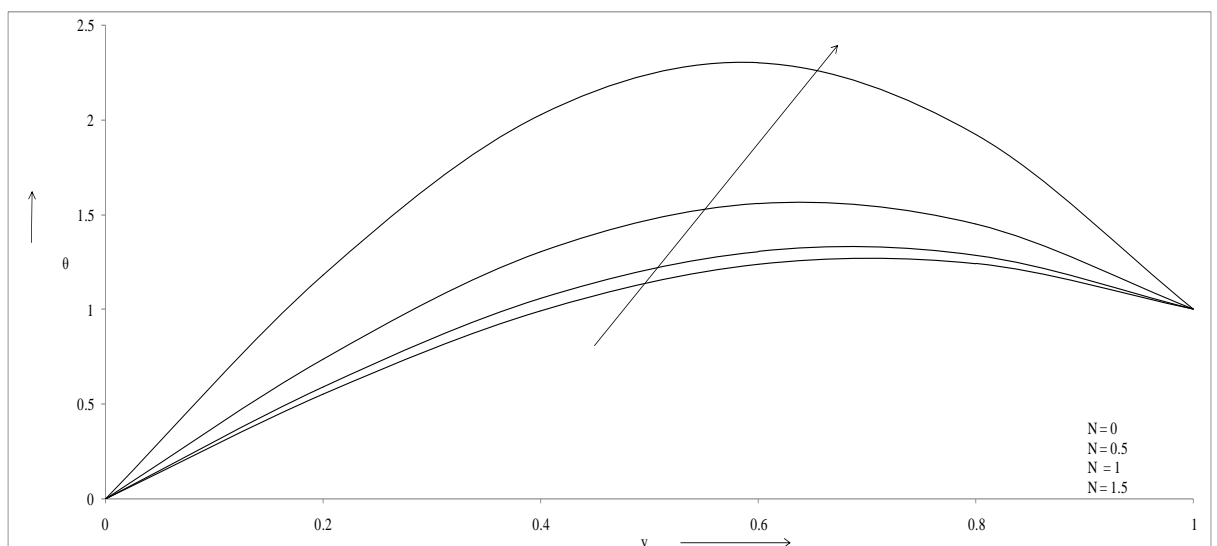


Figure 10. Temperature profiles versus y for different values of N when $Gr=10$, $Gc=10$, $Re=2$, $Ha=1.0$, $Pe=0.71$, $S=5.0$, $Sc=0.60$, $J=0.5$, $\omega=0.1$, $\epsilon=0.001$, $t=0.5$, $\lambda_1=0.1$.

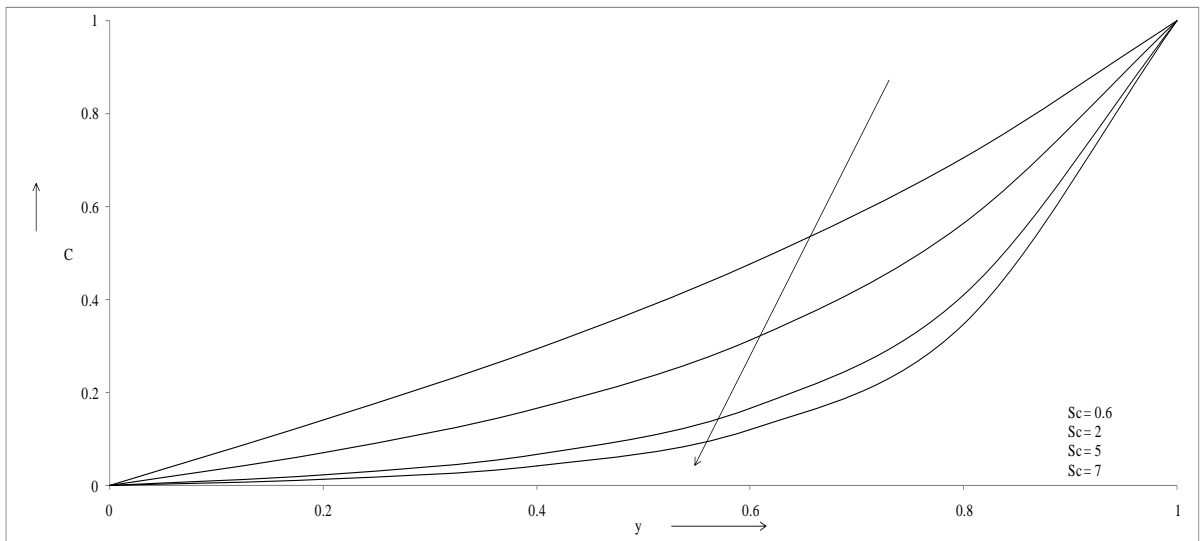


Figure 11. Concentration profiles versus y for different values of Sc when $Gr=10$, $Gc=10$, $Re=2$, $Ha=1.0$, $Pe=0.71$, $S=5.0$, $N=1.0$, $J=0.5$, $\omega=0.1$, $\epsilon=0.001$, $t=0.5$, $\lambda_1=0.1$.

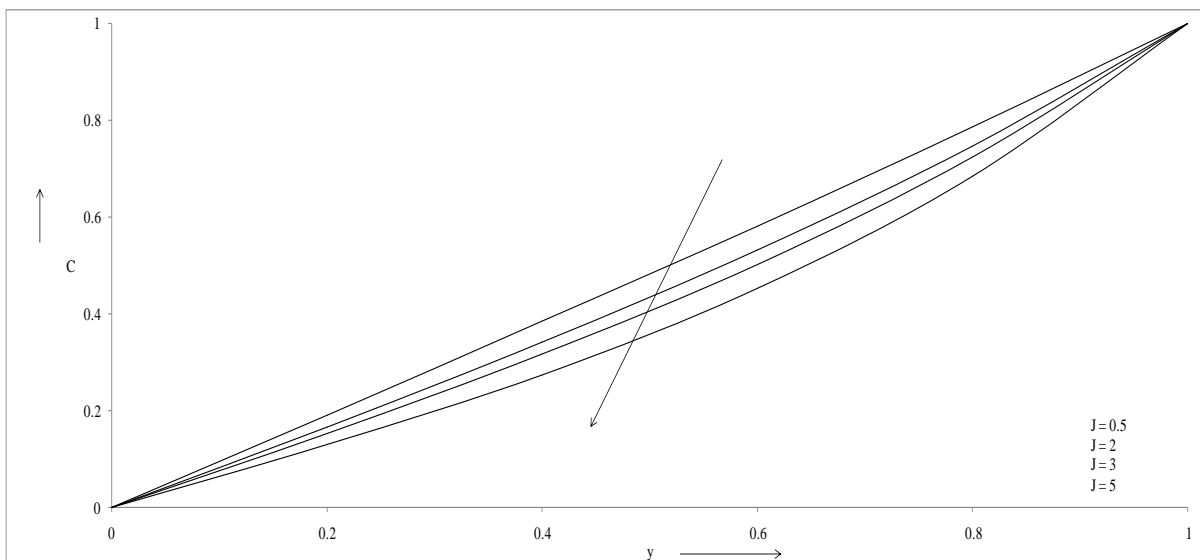


Figure 12. Concentration profiles versus y for different values of J when $Gr=10$, $Gc=10$, $Re=2$, $Ha=1.0$, $Pe=0.71$, $S=5.0$, $N=1.0$, $Sc=0.60$, $\omega=0.1$, $\epsilon=0.001$, $t=0.5$, $\lambda_1=0.1$.

Table 1. Velocity profiles with y for different values of Re when $Gr=10$, $Gc=10$, $Ha=1.0$, $Pe=0.71$, $S=5.0$, $N=1.0$, $Sc=0.60$, $J=4$, $\omega=1$, $\epsilon=0.001$, $t=0.5$, $\lambda_1=0.1$.

y	$Re=1$	$Re=5$	$Re=10$	$Re=20$
0	0	0	0	0
0.2	1.2938	1.2937	1.2933	1.2928
0.4	2.2628	2.2627	2.2620	2.2613

0.6	2.6372	2.6370	2.6364	2.6356
0.8	2.2405	2.2404	2.2400	2.2395
1	1.0008	1.0008	1.0008	1.0008

Table 2. Velocity profiles with y for different values of Pe when $Gr=10$, $Gc=10$, $Re=2$, $Ha=1.0$, $S=5.0$, $N=1.0$, $Sc=0.60$, $J=4$, $\omega=1$, $\epsilon=0.001$, $t=0.5$, $\lambda_1=0.1$.

y	Pe=0.71	Pe=10	Pe=15	Pe=30
0	0	0	0	0
0.2	1.29383	1.29312	1.29304	1.29298
0.4	2.2629	2.26176	2.26162	2.26151

Table 3. Velocity profiles versus y for different values of ω when $Gr=10$, $Gc=10$, $Re=2$, $Ha=1.0$, $Pe=0.71$, $S=5.0$, $N=1.0$, $Sc=0.60$, $J=4$, $\varepsilon=0.001$, $t=0.5$, $\lambda_1=0.1$.

y	$\omega=1$	$\omega=3$	$\omega=5$	$\omega=8$
0	0	0	0	0
0.2	1.2938	1.2934	1.2930	1.2924
0.4	2.2629	2.2622	2.2613	2.2603
0.6	2.6372	2.6363	2.6351	2.6339
0.8	2.2405	2.2395	2.2383	2.2374
1	1.0008	1.0000	0.9992	0.9993

Table 5. Temperature profiles versus y for different values of ω when $Gr=10$, $Gc=10$, $Re=2$, $Ha=1.0$, $Pe=0.71$, $S=5.0$, $N=1.0$, $Sc=0.60$, $J=4$, $\varepsilon=0.001$, $t=0.5$, $\lambda_1=0.1$.

y	$\omega=1$	$\omega=3$	$\omega=5$	$\omega=8$
0	0	0	0	0
0.2	0.7380	0.7377	0.7373	0.7369
0.4	1.3024	1.3019	1.3011	1.3005
0.6	1.5604	1.5597	1.5588	1.5581
0.8	1.4513	1.4505	1.4495	1.4491
1	1.0008	1.0000	0.9992	0.9993

Table 7. Numerical values of skin friction coefficient at the plates for different values of physical parameters

Gr	Gc	Re	Ha	Pe	S	N	Sc	J	ω	λ_1	τ_0	τ_1
10	10	2	1	0.71	5	1	0.6	4	1	0.1	6.7495	-8.3132
10	10	2	1	0.71	5	0	0.6	4	1	0.1	5.71417	-7.2383
10	10	2	1	0.71	5	0.5	0.6	4	1	0.1	5.93043	-7.4643
10	10	2	1	0.71	5	1.5	0.6	4	1	0.1	9.17093	-10.787

0.6	2.63723	2.63609	2.63594	2.63581
0.8	2.24053	2.23983	2.23974	2.23964
1	1.00088	1.00088	1.00088	1.00088

Table 4. Temperature profiles versus y for different values of Pe when $Gr=10$, $Gc=10$, $Re=2$, $Ha=1.0$, $S=5.0$, $N=1.0$, $Sc=0.60$, $J=4$, $\omega=1$, $\varepsilon=0.001$, $t=0.5$, $\lambda_1=0.1$.

y	Pe=0.7	Pe=10	Pe=15	Pe=30
0	0	0	0	0
0.2	0.7380	0.7373	0.7373	0.7372
0.4	1.3024	1.3014	1.3012	1.3011
0.6	1.5604	1.5594	1.5592	1.5590
0.8	1.4513	1.4507	1.4506	1.4505
1	1.0008	1.0008	1.0008	1.0008

Table 6. Concentration profiles versus y for different values of ω when $Gr=10$, $Gc=10$, $Re=2$, $Ha=1.0$, $Pe=0.71$, $S=5.0$, $N=1.0$, $Sc=0.60$, $J=4.0$, $\varepsilon=0.001$, $t=0.5$, $\lambda_1=0.1$.

y	$\omega=1$	$\omega=3$	$\omega=5$	$\omega=8$
0	0	0	0	0
0.2	0.1402	0.14011	0.14	0.13994
0.4	0.29396	0.29377	0.29353	0.29343
0.6	0.47616	0.47584	0.47545	0.47533
0.8	0.70444	0.70392	0.70332	0.70327
1	1.00088	1.00007	0.9992	0.99935

10	10	2	1	0.71	1	1	0.6	4	1	0.1	4.20589	-5.6234
10	10	2	1	0.71	2	1	0.6	4	1	0.1	4.55898	-6.0102
10	10	2	1	0.71	3	1	0.6	4	1	0.1	5.03612	-6.5228
10	10	2	1	0.71	5	1	0.6	4	3	0.1	6.74776	-8.3116
10	10	2	1	0.71	5	1	0.6	4	5	0.1	6.74531	-8.3081
10	10	2	1	0.71	5	1	0.6	4	8	0.1	6.74229	-8.3014
10	10	2	1	0.71	5	1	0.6	4	1	0.2	7.21019	-9.0917
10	10	2	1	0.71	5	1	0.6	4	1	0.5	8.53872	-11.367
10	10	2	1	0.71	5	1	0.6	4	1	1	10.5884	-14.976
10	10	2	1	0.71	5	1	2	4	1	0.1	6.29331	-7.7241
10	10	2	1	0.71	5	1	5	4	1	0.1	5.92041	-7.1451
10	10	2	1	0.71	5	1	7	4	1	0.1	5.81299	-6.9376
10	10	2	1	0.71	5	1	0.6	2	1	0.1	6.9119	-8.5086
10	10	2	1	0.71	5	1	0.6	3	1	0.1	6.8263	-8.4063
10	10	2	1	0.71	5	1	0.6	5	1	0.1	6.68025	-8.2282
10	10	2	1	10	5	1	0.6	4	1	0.1	6.74572	-8.3095
10	10	2	1	15	5	1	0.6	4	1	0.1	6.74527	-8.309
10	10	2	1	30	5	1	0.6	4	1	0.1	6.745	-8.3085
10	10	2	2	0.71	5	1	0.6	4	1	0.1	4.94973	-5.8202
10	10	2	3	0.71	5	1	0.6	4	1	0.1	3.35551	-3.2195
10	10	2	4	0.71	5	1	0.6	4	1	0.1	2.26605	-0.9481
1	10	2	1	0.71	5	1	0.6	4	1	0.1	2.5615	-2.3153
2	10	2	1	0.71	5	1	0.6	4	1	0.1	3.02683	-2.9817
3	10	2	1	0.71	5	1	0.6	4	1	0.1	3.49216	-3.6482
10	1	2	1	0.71	5	1	0.6	4	1	0.1	5.61765	-5.6203
10	2	2	1	0.71	5	1	0.6	4	1	0.1	5.74342	-5.9195
10	3	2	1	0.71	5	1	0.6	4	1	0.1	5.86918	-6.2188
10	10	5	1	0.71	5	1	0.6	4	1	0.1	6.74884	-8.3128
10	10	10	1	0.71	5	1	0.6	4	1	0.1	6.7468	-8.311
10	10	20	1	0.71	5	1	0.6	4	1	0.1	6.74434	-8.3085

Table 8. Numerical values of Nusselt number at the plates for different values of physical parameters

Pe	S	N	ω	Nu ₀	Nu ₁
0.71	5	1	0.1	-3.8422	2.95814

10	5	1	0.1	-3.842	2.95789
15	5	1	0.1	-3.8416	2.95757
20	5	1	0.1	-3.8412	2.95718
0.71	0	1	0.1	-1.1896	-0.6427
0.71	1	1	0.1	-1.4332	-0.2235
0.71	2	1	0.1	-1.7566	0.28203
0.71	3	1	0.1	-2.2017	0.91623
0.71	5	0	0.1	-2.845	1.75614
0.71	5	0.5	0.1	-3.0521	2.01362
0.71	5	1.5	0.1	-6.2092	5.59377
0.71	5	1	1	-3.842	2.95812
0.71	5	1	1.5	-3.8418	2.95809
0.71	5	1	2	-3.8415	2.95803

Table 9. Numerical values of Sherwood number at the plates for different values of physical parameters

Sc	J	ω	Sh ₀	Sh ₁
0.6	4	1	-0.6899	-1.697
0.6	4	3	-0.6895	-1.6953
0.6	4	5	-0.6889	-1.6937
2	4	1	-0.3358	-2.8506
5	4	1	-0.1023	-4.477
7	4	1	-0.0533	-5.2961
0.6	2	1	-0.8256	-1.3724
0.6	3	1	-0.7536	-1.5397
0.6	5	1	-0.6333	-1.8455

5. Conclusions:

Effect of heat and mass transfer on unsteady MHD oscillatory flow of Jeffrey fluid between parallel plates in the presence of chemical reaction and heat source is investigated. The velocity, temperature and concentration profiles are obtained and shown through graphs, dimensionless shear stress, rate of heat and mass transfer at the plates are derived and their numerical values are presented through tables. In view of the above, the following conclusions are made

- (i) The velocity and temperature of the fluid increases as the heat source parameter or radiation parameter.
- (ii) The velocity and temperature of the fluid decrease with the increase of Peclet number or frequency of the oscillation.
- (iii) Due to increase in Schmidt number, chemical reaction parameter or frequency of the oscillation, the velocity and concentration of the fluid decrease.
- (iv) As Grashof number, modified Grashof number, heat source parameter, radiation parameter or material parameter increases the skin-friction coefficient increases at the plate (when $y = 0$) while decreases at the plate (when $y = 1$).
- (v) An increase in Reynolds number, Hartmann number, Peclet number or Schmidt number causes an increase in skin-friction coefficient at the plate (when $y = 1$), while it decreases at the plate (when $y = 0$).
- (vi) The rate of heat transfer at the plate (when $y = 0$) increases due to increase in Peclet number or frequency of the oscillation, while it decreases as the heat source parameter or radiation parameter increases.
- (vii) The rate of heat transfer at the plate (when $y = 1$) increases due to increase in heat source parameter or radiation parameter while it decreases due to increase in Peclet number or frequency of the oscillation.
- (viii) Due to increase in frequency of the oscillation, the rate of mass transfer increases at both the plates.
- (ix) An increase in Schmidt number or chemical reaction parameter leads to an increase in the rate of mass transfer at the plate (when $y = 0$), while it decreases at the plate (when $y = 1$).

6. References:

1. Acharya, M; Dash, G. C. and Singh, L. P., "Magnetic field effects on the free convection and mass transfer flow through porous medium with constant suction and constant heat flux". Indian J. Pure Appl. Math., Vol. 31, 2000, pp. 1-8.
2. Asadullah, M.; Umar, K.; Nareed, A.; Raheela, M. and Mohyuddin, S. T., "MHD flow of a Jeffrey fluid in converging and diverging channels". Int. J. Mod. Math. Sci., Vol. 6, 2013, pp. 92-106.

3. Bakr, A. A., "Effects of chemical reaction on MHD free convection and mass transfer flow of a micropolar fluid with oscillatory plate velocity and constant heat source in a rotating frame of reference". *Comm. Nonlinear Sci. Num. Simulat.*, Vol. 16, 2011, pp. 698-710.
4. Bejan, A. And Khair, K. R., "Heat and mass transfer by natural convection in a porous medium". *Int. J. Heat Mass Transfer*, Vol. 28, 1985, pp. 909-918.
5. Chamkha, A. J., "MHD flow of a numerical of uniformly stretched vertical permeable surface in the presence of heat generation/absorption and chemical reaction". *Int. Comm. Heat Mass transfer*, Vol. 30, 2003, pp. 413-422.
6. Deka, R.; Das, U. N. and Soundalgekar, V. M., "Effect of mass transfer on flow past an impulsively started infinite vertical plate with constant heat flux and chemical reaction". *Forschung Ingenieurwesen*, Vol.60, 1994, pp. 284-287.
7. Devika, B.; Satya Narayana, P. V. And Venkataramana, S., "MHD oscillatory flow of a visco elastic fluid in a porous channel with chemical reaction". *Int. J. of Engg. Sci. Invention*, Vol. 2, 2013, pp. 26-35.
8. Israel-Cookey, C. and Nwaigwe, C., "Unsteady MHD flow of a radiating fluid over a moving heated porous plate with time-dependent suction". *Am. J. Sci. Ind. Res.*, Vol. 1, 2010, pp. 88-95.
9. Kavita, K.; Prasad, R. K. and Kumari, B. A., "Slip effects on MHD oscillatory flow of Jeffrey fluid in a channel with heat transfer". *Int. J. Math. Arch.*, Vol. 3, 2012, pp. 2903-2911.
10. Kavita, K.; Prasad, R. K. and Kumari, B. A., "Influence of heat transfer on MHD oscillatory flow of Jeffrey fluid in a channel". *Adv. Appl. Sci. Res.*, Vol. 3, 2012, pp. 2312-2325.
11. Kim, U. J., "Unsteady MHD convective heat transfer past a semi infinite vertical porous moving plate with variable suction". *Int. J. Eng. Sci.* Vol. 38, 2000, pp. 833-845.
12. Kumar, N; Jain, T. and Gupta, S., "Unsteady MHD free convection flow through porous medium sandwiched between viscous fluids". *Int. J. Ener. Tech.*, Vol. 4, 2012, pp. 1-11.
13. Makinde, O. D. and Mhone, P. Y., "Heat transfer to MHD oscillatory flow in a channel filled with porous medium". *Romanian J. Physics*, Vol. 50, 2005, pp. 931-938.
14. Pal, D. and Talukdar, B., "Perturbation analysis of unsteady magnetohydrodynamic convective heat and mass transfer in a boundary layer slip flow past a vertical permeable plate with thermal radiation and chemical reaction". *Communications in Nonlinear Science and Numerical Simulation*, Vol. 15, 2010, pp. 1813-1830.
15. Sharma, P. R. and Singh, G., "Effects of variable thermal conductivity and heat source/sink on MHD flow near a stagnation point on a linearly stretching sheet". *J. of appl. fluid mechanics*, Vol. 2, 2008, pp. 13-22.
16. Sharma, P.R. and Sharma, M.K., "Unsteady flow and heat-transfer between two parallel plates". *Bull. Pure Appl. Science, India*, Vol.16, 1997, pp. 183-198.

17. Sharma, P.R. and Kumar, N., "Unsteady flow and heat transfer between two horizontal plates in the presence of transverse magnetic field". Bull. Pure Appl. Science, India, Vol. 17E, 1998, pp. 39-49.
18. Sharma, P.R. and Chaturvedi, R., "Unsteady flow and heat transfer of an electrically conducting viscous incompressible fluid between two non-conducting parallel porous plates under uniform transverse magnetic field". "Ganita Sandesh" J. Raj.Ganita Parishad, India, Vol.17, 2003, pp.9-14.
19. Sharma, P.R.; Chawla, S. and Singh, R. "Unsteady plane poiseuille flow and heat transfer in the presence of oscillatory temperature of the lower plate". Indian J. Theo. Phys., Vol. 52, 2005, pp. 215-226.
20. Shateyi, S. and Motsa, S., "Unsteady magnetohydrodynamic convective heat and mass transfer past an infinite vertical plate in a porous medium with thermal radiation heat generation/absorption and chemical reaction". Advanced Topics in Mass Transfer, ISBN: 978-953-307-333-0, 2011, pp. 145-162.
21. Sreenadh, S., Devaki, P. and Diwakar, R., " Unsteady flow of Jeffrey in an elastic tube with a stenosis". Int. Conf. of Fluid Dynamics and Thermodynamics Technologies, Vol. 33, 2012, pp. 136-142.
22. Vineet, K. S.; Gupta, P. C. and Varshney, N. K., "MHD effects on free convection fluid flow past a vertical surface with porous medium and radiation". Int. J. Math. Analysis, Vol. 6, 2012, pp. 29-37.